

CHEMICAL REACTOR DESIGN FOR PROCESS PLANTS

Volume Two: Case Studies and Design Data

HOWARD F. RASE

**W. A. Cunningham Professor of Chemical Engineering
The University of Texas at Austin**

Original Illustrations by

JAMES R. HOLMES

**Associate Professor of Engineering Graphics
The University of Texas at Austin**

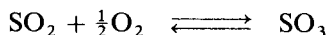
A WILEY-INTERSCIENCE PUBLICATION

JOHN WILEY & SONS, New York • London • Sydney • Toronto

CASE STUDY 107

Sulfur Dioxide Oxidation

THERE EXISTS no better opportunity than SO_2 oxidation to demonstrate the complexity and problems that confront the designer in developing adequate and meaningful design models. Superficially, the system presents the classically simple case of an adiabatic single reaction with negligible side reaction. Precise physical and thermodynamic data exist (10).



As will be seen, however, the reaction is mechanistically complex, exhaustive studies have produced no general agreement on acceptable rate forms, and the active catalytic component is in the molten state at operating conditions. This latter fact can cause the apparent effective diffusivity to change markedly with temperature depending on the way the liquid distributes within the pores (see p. 148¹).

Problem Statement

The following are typical data obtained from a commercial sulfuric-acid plant converter using sludge acid as the feed to the burner that precedes the converter.

Reactor diameter: 35 ft

Feed composition to converter:

Component	Mole %
SO_2	6.26
O_2	8.30
CO_2	5.74
N_2	79.70
	100.00

Feed rate: 10,858 lb moles/hr

Bed No.	Temperature, °F		Exit Conversion	Catalyst Height, ft	Inlet Pressure In. H ₂ O
	In	Out			
1	867	1099	68.7	1.276	63
2	851	923	91.8	1.408	51
3	858	869	96.0	1.511	41
4	815	819	97.5	1.848	36

Develop a model useful for design purposes that will predict bed heights and produce reasonable agreement with this and other similar operating data.

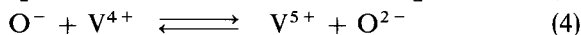
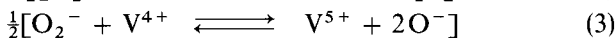
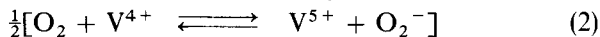
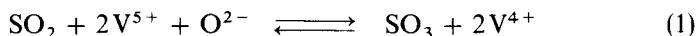
Catalyst Properties

	Wt. %	Mole Ratio Comp/V ₂ O ₅
V ₂ O ₅	8.2	
K ₂ O	12.3	2.9
Na ₂ O	1.2	0.43
Fe ₂ O ₃	1.0	
$S_g = 1-2 \text{ m}^2/\text{g}$		$\rho_b = 0.567 \text{ g/cc}$
$V_p = 0.35 \text{ cc/g}$		$\rho_p = 1.1729 \text{ g/cc}$
Size 0.22 in. \times 0.40 in. cylinders		

Kinetics and Mechanism

The many rate equations that have been proposed over the years for this interesting vanadium pentoxide catalyst have been reviewed (1-3,8,14). Most of the commercial catalysts are supported on some type of siliceous material, such as kieselguhr. Variations in preparing the support can account for much of the apparent inconsistency in rate data gathered on pelleted catalysts. Quite obviously, the effectiveness factors of different forms of apparently similar catalysts can vary greatly. More recent studies using finely ground catalyst have eliminated intraparticle diffusion as a variable and brought more consistency in the rate data and mechanistic arguments. It is now generally agreed that the mechanism involves oxidation-reduction of active V₂O₅ that exists on the support at operating conditions in the molten state (3-5,14).

Various schemes have been proposed. The following is typical (9).



Various rate equations can be derived based on this mechanistic scheme and the designated rate-controlling step. Using fine catalyst, for which the effectiveness factor is unity, it has been shown that the rate equation based on Eq. 3 being the slow step with 1, 2, and 4 at equilibrium fits the data most successfully in the range above 30% conversion (9).

Although this equation correlates data in the range above 30% conversion very well, it is not satisfying for modeling because it is indeterminant at the limit of zero partial pressure of SO_3 . An alternate equation that does not suffer this weakness involves similar arguments, but uses a different mechanism (5).

With reactions 2 and 3 combined ($\frac{1}{2}\text{O}_2 + \text{V}^{4+} \xrightleftharpoons{k_5} \text{V}^{5+} + \text{O}^-$) as rate controlling and reactions 1 and 4 at equilibrium, a straightforward derivation yields (3,5,9)

$$(-\hat{r}_{\text{SO}_2}) = \psi \eta \hat{k}_{pm} \frac{K_M P_{\text{SO}_2} / P_{\text{SO}_3}}{[1 + (K_M P_{\text{SO}_2} / P_{\text{SO}_3})^{\frac{1}{2}}]^2} \left[P_{\text{O}_2} - \left(\frac{P_{\text{SO}_3}}{P_{\text{SO}_2} K_p} \right)^2 \right] \quad (\text{CS-7.1})$$

or

$$(-\hat{r}_{\text{SO}_2}) = \psi \eta \hat{k}_{pm} \frac{K_M P_{\text{SO}_2}}{[P_{\text{SO}_3}^{\frac{1}{2}} + (K_M P_{\text{SO}_2})^{\frac{1}{2}}]^2} \left[P_{\text{O}_2} - \left(\frac{P_{\text{SO}_3}}{P_{\text{SO}_2} K_p} \right)^2 \right] \quad (\text{CS-7.2})$$

Rate units are g moles SO_2 conv/(g cat.)(hr), $K_M = K_1 C_{\text{O}_2^-}$, and $\hat{k}_{pm} = k_p C_v^2$, where C_v^2 is the total vanadium concentration. Equation CS-7.1 fits the same experimental data with satisfactory precision (7) and has recently been demonstrated in a separate study on fine catalyst (14) to fit data over a wide temperature range better than any of the eleven other equations tested.

The value of K_M is agreed to be somewhat insensitive to catalyst receipt in the low range (3,5,7). But a study of a variety of catalysts with varying Na_2O content indicates Na_2O content to be an important variable related to \hat{k}_{pm} , as shown in Fig. 1.5, p. 27¹, (7). Conveniently, these data for fine catalyst of unit effectiveness factor exhibit an isokinetic point. Thus E is a function of A , and the best fit for the data can be selected by trying different reasonable values of E ; From Fig. 1.5, $\ln A = 7.108707 \times 10^{-4} E - 1.365433$. The emphasis on reasonable is essential to prevent any such effort from being a curve fitting expedition glossed over with a veneer of theory. For the model to have predictive value, it must be consistent with physical reality. In this

case that means E should lie somewhere between curves 1 and 2 ($E = 41,400$ – $53,800$), which is in the range of Na_2O content of interest. Interpolating for the catalyst in question $E \cong 47,000 \text{ cal/(g-mole)}(^{\circ}\text{K})$.

Effectiveness Factor

The complexity of the rate form suggests the need for deriving an effectiveness factor based on this form. A rather thorough study of effectiveness factors for the type catalyst being considered has been presented, but a simpler rate form applicable over modest ranges of conversion was used and an effectiveness factor derived as follows (6,12,13).

$$(-\hat{r}_{\text{SO}_2}) = \hat{k}_p \left(P_{\text{SO}_2} P_{\text{O}_2}^{\frac{1}{2}} - \frac{P_{\text{SO}_3}}{K_p} \right) \quad (\text{CS-7.3})$$

Mass-Transfer Balances for Spherical Particle ($P = 1 \text{ Atm}$)

$$\frac{d}{dr_I} \left(r_I^2 \mathcal{D}_{\text{ISO}_2} \frac{dy_{\text{SO}_2}}{dr_I} \right) - r_I^2 (-\hat{r}_{\text{SO}_2}) RT \rho_p = 0 \quad (\text{CS-7.4})$$

$$\frac{d}{dr_I} \left(r_I^2 \mathcal{D}_{\text{IO}_2} \frac{dy_{\text{O}_2}}{dr_I} \right) - r_I^2 \frac{1}{2} (-\hat{r}_{\text{SO}_2}) RT \rho_p = 0 \quad (\text{CS-7.5})$$

$$\frac{d}{dr_I} \left(r_I^2 \mathcal{D}_{\text{ISO}_3} \frac{dy_{\text{SO}_3}}{dr_I} \right) + r_I^2 (-\hat{r}_{\text{SO}_2}) RT \rho_p = 0 \quad (\text{CS-7.6})$$

where r_I is the radial distance in an equivalent sphere.

From stoichiometry and Eqs. CS-7.4–CS-7.6, expressions for y_{SO_3} and y_{O_2} can be obtained in terms of y_{SO_2} upon integrating.

$$y_{\text{O}_2} = (y_{\text{O}_2})_s + \frac{1}{2} \frac{\mathcal{D}_{\text{ISO}_2}}{\mathcal{D}_{\text{IO}_2}} [y_{\text{SO}_2} - (y_{\text{SO}_2})_s] \quad (\text{CS-7.7})$$

$$y_{\text{SO}_3} = (y_{\text{SO}_3})_s - \frac{\mathcal{D}_{\text{ISO}_2}}{\mathcal{D}_{\text{ISO}_3}} [y_{\text{SO}_2} - (y_{\text{SO}_2})_s] \quad (\text{CS-7.8})$$

where suffix s indicates a value measured at the exterior surface of the catalyst. Then Eq. CS-7.4 can be rewritten using Eqs. CS-7.7 and CS-7.8, conversion X , and assuming an isothermal particle

$$\frac{d^2 X}{dr_k^2} + \frac{2y_0}{2 - y_0 X} \left(\frac{dX}{dr_k} \right)^2 + \frac{2}{r_k} \frac{dX}{dr_k} = - \frac{D_p^2 RT (2 - y_0 X)^2}{4(4y_0 - 2y_0^2) \mathcal{D}_{\text{ISO}_2}} \rho_p (-\hat{r}_{\text{SO}_2}) \quad (\text{CS-7.9})$$

where y_0 is the initial mole fraction SO_2 in feed and $r_k = 2r_I/D_p$ similarly values of partial pressures in Eq. CS-7.3 be written in terms of y_0 and X .

Equation CS-7.9 has been solved numerically (13) and $(dX/dr_k)r_k = 1$ evaluated so that the effectiveness factor can be obtained.

$$\eta = \frac{\text{observed rate}}{\text{rate based on concentrations @ exterior surface}}$$

$$= \frac{6y_0(2 - y_0)}{(2 - y_0 X_s)^2} \left(-\frac{dX}{dr_k} \right)_{r_k=1} \frac{1}{\phi_m f(X_s)} \quad (\text{CS-7.10})$$

where

$$\phi_m = \frac{D_p^2 RT \hat{k}_p \rho_p}{4 \mathcal{D}_{\text{ISO}_2} 3600} = 9 \left(\frac{V_k}{a_p} \right)^2 \frac{RT \hat{k}_p \rho_p}{(\mathcal{D}_{\text{ISO}_2})(3600)} \quad (\text{CS-7.11})$$

$f(X)_s$ is the rate equation in X and y_0 without \hat{k}_p ; \hat{k}_p is the rate constant based on Eq. CS-7.3, g moles/(g cat.)(hr)(atm)^{1.5}, V_k is the particle volume; and $R = 82.06$. The RT term converts \hat{k}_p to required concentration units.

The solution was rather insensitive to conversion and feed composition, and a convenient empirical formula for η as a function of ϕ_m was obtained from the calculated data.

$$\eta = (\phi_m + C_1)/(A_1 \phi_m + B_1) \quad \text{for } 3 < \phi_m < 400 \quad (\text{CS-7.12})$$

$$A_1 = 8.52518$$

$$B_1 = 539.706$$

$$C_1 = 503.004$$

$$\eta = A_2(\phi_m)^{B_2} \quad \text{for } \phi_m > 400 \quad (\text{CS-7.13})$$

$$A_2 = 3.8299$$

$$B_2 = -0.46748$$

Since all this work has been already accomplished, it seems reasonable to apply it directly in the computational program, by calculating the rate at any point first using Eq. CS-7.1 with $\eta = 1.0$. Then equate that rate to Eq. CS-7.3 and solve for \hat{k}_p in Eq. CS-7.3 for use in Eqs. CS-7.11–CS-7.13.

An effective diffusivity for use in Eq. CS-7.9 was determined from the extensive experimental data reported on a catalyst similar to the subject catalyst (12).

$$\mathcal{D}_{\text{ISO}_2} = 0.0286 \text{ cm}^2/\text{sec}$$

Reactor Model

This reactor is a typical multibed adiabatic reactor with intermediate cooling. Given good thermodynamic data, which are existent for this system (10), it should be possible to calculate adiabatic temperatures for the observed

outlet conversions that agree with measured values for each bed provided temperatures and compositions are determined accurately. Since in the first bed, particularly, catalyst surface temperatures will be greater than bulk temperatures, thermocouples must not touch the catalyst. A location just above the bed on the inlet and at the inert support-catalyst interface at the outlet have been recommended (11). Precise methods for analysis are also suggested (11).

Since SO_2 converters operate near atmospheric pressure and do not require high velocities for exterior heat transfer, it is only necessary to minimize pressure drop in order to minimize power consumption. Thus these converters are designed for low mass velocities with only about $\frac{1}{2}$ –1 in. of H_2O $\Delta P/\text{ft}$ of bed. For this reason, unlike high-pressure adiabatic reactors where larger ΔP s are permissible, interfacial gradients between the catalyst surface and the bulk phase will occur in the first bed because of high rates. Accordingly, equations for this phenomenon will be included.

Design Equations

Basis: 1 mole of feed

$$\frac{dn_{\text{SO}_2}}{dZ} = \frac{\rho_b(-\hat{r}_{\text{SO}_2})M_F}{G} \quad \text{or} \quad \Delta Z = \frac{\Delta n_{\text{SO}_2} G}{\rho_b(-\hat{r}_{\text{SO}_2})M_F}$$

$$d(\sum n_j H_j) = (-\Delta H_{\text{SO}_2})dn_{\text{SO}_2} \quad \text{or} \quad \Delta n_{\text{SO}_2} = \frac{\sum n_j \Delta H_j}{(-\Delta H_{\text{SO}_2})}$$

where n_j is the moles of component j per mole of total feed and H_j is the enthalpy of any component j .

$$k_{g_j} a_m [(P_j)_b - (P_j)_s] = (-\hat{r}_{\text{SO}_2}) \quad \text{integrate mass eq. to rate of rxn}$$

$$h a_m (T_s - T_b) = (-\hat{r}_{\text{SO}_2})(-\Delta H_{\text{SO}_2})$$

where $a_m = a_p/V_k \rho_b$, b indicates bulk conditions, and s indicates surface conditions.

Algorithm

1. Select a temperature increment (1°F was found satisfactory).
2. Calculate ΔH_{SO_2} @ $T_n + \Delta T$

$$\Delta H_{\text{SO}_2} = a + bT + cT^2 + dT^3 *$$

$$a = 4.1923286 \times 10^4$$

$$b = -64.3951192$$

$$c = 7.52214287 \times 10^{-2}$$

$$d = -2.94166667 \times 10^{-5}$$

* Based on curve fits of tabular data (10).

3. Calculate H_j 's @ T_n and $T_n + \Delta T$

$$H_j = a' + b'T + c'T^2 + d'T^3$$

Basis: enthalpy above 298°K*

	a'	b'
SO ₂	-2.651×10^3	7.41333334
SO ₃	-3.4906571×10^3	9.16952383
O ₂	-1.8469429×10^3	5.6429762
N ₂	-1.9181143×10^3	6.27571429
CO ₂	-2.0802286×10^3	5.59059524
	c'	d'
	4.8×10^{-3}	$-1.33333333 \times 10^{-6}$
	$7.73571428 \times 10^{-3}$	$-2.1666666 \times 10^{-6}$
	$2.21428571 \times 10^{-3}$	-5.833333×10^{-7}
	$7.71428566 \times 10^{-4}$	$2.3925238 \times 10^{-15}$
	$5.89285714 \times 10^{-3}$	$-1.4166667 \times 10^{-6}$

4. Calculate $\Sigma n_j \Delta H_j = \Sigma n_j (H_{jT_n + \Delta T} - \Delta H_{jT_n})$

5. Calculate $\Delta n_{\text{SO}_2} = \frac{\Sigma n_j \Delta H_j}{(-\Delta H_{\text{SO}_2})}$

6. Calculate conversion $X_{n+1} = \frac{(n_{\text{SO}_3})_n + \Delta n_{\text{SO}_2}}{(n_{\text{SO}_2})_0}$

7. Calculate moles each component per mole of feed

$$(n_{\text{SO}_2})_{n+1} = (n_{\text{SO}_2})_n - \Delta n_{\text{SO}_2}$$

$$(n_{\text{SO}_3})_{n+1} = (n_{\text{SO}_3})_n + \Delta n_{\text{SO}_2}$$

$$(n_{\text{O}_2})_{n+1} = (n_{\text{O}_2})_n - \frac{1}{2} \Delta n_{\text{SO}_2}$$

$$(n_{\text{T}})_{n+1} = (n_{\text{SO}_2})_{n+1} + (n_{\text{SO}_3})_{n+1} + (n_{\text{O}_2})_{n+1} + (n_{\text{CO}_2})_0 + (n_{\text{N}_2})_0$$

8. Calculate mole fractions

$$(y_{\text{SO}_2})_{n+1} = \frac{(n_{\text{SO}_2})_{n+1}}{(n_{\text{T}})_{n+1}}, \text{ etc.}$$

* Based on curve fits of tabular data (10).

9. Calculate average mole fractions for increment and average molecular weight (M_m)

$$\bar{y}_{\text{SO}_2} = \frac{(y_{\text{SO}_2})_n + (y_{\text{SO}_2})_{n+1}}{2}, \text{ etc.}$$

$$M_m = \sum \bar{y}_j MW$$

10. Calculate average bulk partial pressures for increment

$$\bar{P}_{\text{SO}_2} = \bar{y}_{\text{SO}_2} P, \text{ etc.}$$

11. (a) Calculate rate based on known conditions using Eq. CS-7.1 with $\psi = 1$ and $\eta = 1$.

$$\hat{k}_{p_m} = A \exp\left(-\frac{E}{R'T}\right), \frac{\text{g moles SO}_2}{(\text{g cat.})(\text{hr})(\text{atm})}$$

$$\ln A = 7.108707 \times 10^{-4} E - 1.365433$$

$$K_m = 2.3 \times 10^{-8} \exp\left(\frac{27,200}{R'T}\right)$$

$$\log_{10} K_p = \frac{5.14488992 \times 10^3}{T} - 4.8882412^*$$

η is determined from Eqs. CS-7.11-CS-7.13.

- (b) Calculate value of \hat{k}_p from

$$(-\hat{r}_{\text{SO}_2}) = \hat{k}_p \left(P_{\text{SO}_2} P_{\text{O}_2}^{\frac{1}{2}} - \frac{P_{\text{SO}_3}}{K_p} \right)$$

- (c) Calculate ϕ_m and η

- (d) Calculate new value of rate by correcting original value by multiplying by η .

12. Calculate surface temperature

$$T_s = \frac{(-\hat{r}_{\text{SO}_2})(-\Delta H_{\text{SO}_2})}{ha_m} + T_b$$

If $T_s - T_b = 2$ or less, go to step 15. If greater than 2, proceed to step 13.

13. Calculate surface partial pressures

$$(P_j)_b - (P_j)_s = \frac{(n)(-\hat{r}_{\text{SO}_2})}{k_{g_j}^s a_m}$$

$n = 1$ for SO_2 , 0.5 for O_2 , and -1 for SO_3 .

* Curve fit from Ref. 10.

31.88
 $\ln k_p = \ln A - E/RT$
 $= 32.04$
 $\log = 9.46$

14. Go back to step 11.
15. Calculate ΔZ and Z

$$\Delta Z = \frac{\Delta n_{\text{SO}_2} G}{\rho_b (-\hat{r}_{\text{SO}_2}) M_F}$$

16. Go to desired conversion. Then proceed to next bed.

Operating inlet pressure was used at the inlet of each bed and pressure was corrected for ΔP loss for each increment using Eq. 11.8B. With appropriate values of the parameters for catalyst. Values for $k_{g_j}^s$ and h were obtained using Eqs. 11.12 and 11.15-16 with $N_{\text{Pr}}^{\frac{2}{3}} = 0.8$ and $(N_{\text{Sc}})^{\frac{1}{3}} = 1.334, 1.272,$ and 1.041 for SO_3 , SO_2 , and O_2 , respectively. Viscosities of the mixture were determined from

$$\mu_m = \frac{\sum_{j=1}^n [\bar{y}_j \mu_j (M_j)^{0.5}]}{\sum_{j=1}^n [\bar{y}_j (M_j)^{0.5}]}$$

$$\mu_j = \exp(\bar{A} + \bar{B}T)$$

	\bar{A}	\bar{B}
SO_2	-5.012	0.0020196
SO_3	-4.855	0.0020196
O_2	-4.172	0.001213
N_2	-4.65	0.002032
CO_2	-4.0571	8.57×10^{-4}

$1.24/27$

$g/m.s$

Results

Because of the lack of experimental data for the catalyst used in the commercial reactor, an effective diffusivity was determined using experimental reaction-rate data reported in the literature (12). This value ($0.286 \text{ cm}^2/\text{sec}$), though based on data obtained in the temperature range of $860\text{--}968^\circ\text{F}$, was used for all four beds. The predicted lengths for beds 1 and 4 were not acceptable (Table CS-7.1) although values for bed 2 and 3 are reasonable. The bed length or catalyst volume is the more sensitive parameter, and all calculations were made to the observed conversion for each bed. If one calculates to the known length, the values of conversion thus obtained may appear rather close to the observed value and give a false sense of security concerning the efficacy of the model.

Experimental values of apparent effective diffusivities, which were determined for a different V_2O_5 catalyst than used for rate data, are in the range of bed 4 operating temperature and are approximately 35% of those at

Table CS-7.1 Comparison of Model Predictions with Operating Data^a

No.	Actual Bed Depth, Ft	Operating Temp., °F		Case 1				Case 2			Case 3		
		In	Out	Conv. %	$\mathcal{D}_{\text{ISO}_2}$	Temp. Out, °F	Bed Depth Ft	$\mathcal{D}_{\text{ISO}_2}$	Temp. Out, °F	Bed Depth, Ft	$\mathcal{D}_{\text{ISO}_2}$	Temp. Out, °F	Bed Depth, Ft
1	1.276	867	1099	68.7	0.0286	1090	0.629	0.027	1090	0.641	0.025	1090	0.657
2	1.408	851	923	91.8	0.0286	926	1.518	0.027	927	1.559	0.025	927	1.614
3	1.511	858	869	96.0	0.0286	872	1.431	0.027	872	1.461	0.025	872	1.523
4	1.848	815	819	97.5	0.0286	820	1.191	0.011	820	1.848	0.011	820	1.848

^aE = 47,000.

Temperature into each bed and conversion in and out set at values observed in operating plant.

higher temperatures such as in beds 1–3. Accordingly, it was decided to determine the appropriate value for bed 4 by selecting the one that caused the operating data to be reproduced. Because bed 4 also operates very close to the isokinetic point, it is rather insensitive to the energy of activation used. Thus the best-fit-value of $\mathcal{D}_{\text{ISO}_2} = 0.011 \text{ cm}^2/\text{sec}$ given in case 3 of Table CS-7.1 should be a rather accurate representation of the apparent diffusivity at operating conditions, and it is 38% of that of 0.0286 determined in the 860–968°F range in a separate study (12).

Using the same technique on bed 3 a value of $\mathcal{D}_{\text{ISO}_2} = 0.025 \text{ cm}^2/\text{sec}$ was determined. This value is very close to the value of 0.0286 determined from laboratory reaction rate data from what appears to be a similar catalyst (12). Clearly effective diffusivities in the range 0.025–0.029 are acceptable for beds 2 and 3. There exists no independent evidence that the effective diffusivities at the conditions of beds 1, 2, and 3 would differ, and the value of $\mathcal{D}_{\text{ISO}_2}$ determined in bed 3 was thus also used for beds 1 and 2. The results of the calculations are summarized in Tables CS-7.1–CS-7.3.

The effect of changing both $\mathcal{D}_{\text{ISO}_2}$ and inlet temperatures are illustrated. It is important to recognize that the reported operating temperatures could be in error by 5–10°F. Referring to Table CS-7.3 the effects of small changes in inlet temperature can be rather dramatic depending on the proximity to equilibrium. The temperature sensitivity of bed 2 is seen to be much less

Table CS-7.2 Effect of Inlet Temperature on Bed Depth

Bed No.	Inlet Temperature °F	Calculated Height, Ft
1	857	0.684
	867	0.657
	877	0.644
2	841	1.634
	851	1.614
	855	1.600
	861	1.607
3	848	1.393
	858	1.523
	868	2.040
4	805	1.724
	815	1.848
	825	2.102

$\mathcal{D}_{\text{ISO}_2}$ same as for Case 3, Table CS-7.1.

Table CS-7.3 Effect of Possible Errors in Plant Observations

Bed No.	Actual Bed Depth, Ft	Operating Temp., °F		Conv. %	Altered Conditions			
					Temp. In °F	Calc. Temp. Out, °F	Conv. %	Bed Depth, Ft
1	1.276	867	1099	68.7	867	1099	71.65	0.748
2	1.408	851	923	91.8	857	923	91.85	1.487
3	1.511	858	869	96.0	855	869	96.0	1.459
4	1.848	815	819	97.5	815	820	97.5	1.848

$\mathcal{D}_{1\text{SO}_4}$ same as for Case 3, Table CS-7.1.

than bed 3. The model, once established, could be useful in determining the optimum inlet temperature for each bed.

Table CS-7.3 is the result of some speculative calculations in which the outlet conversion of the first bed was changed to yield the measured outlet temperature, and the inlet temperatures of beds 2 and 3 were altered so that the measured outlet temperatures are obtained. Good agreement again results for beds 2, 3, and 4; but bed 1, though closer to the actual catalyst loading, is still 41% off. It is reasonable to hypothesize that bed 1 becomes partially deactivated during the early hours of start-up. This is not uncommon in the first bed of exothermic adiabatic reactors. This hypothesis must be tested by independent studies of the catalyst.

Improved rate equations, which are appearing in the literature, should be tested. In fact, it has more recently been shown that a simplified model involving liquid phase diffusion in the vanadium oxide melt and homogeneous reaction is satisfactory for the range of temperatures covered by the first three beds in this example (15). In the low temperature range corresponding to the range of the fourth bed ($<435^\circ\text{C}$), preliminary experimental evidence suggests rather profound changes in catalyst composition when passing between kinetic and diffusion-controlled regimes (15). We are realizing that SO_2 oxidation, which initially appeared to be a rather simple reaction system, is really quite complex; and it has become a dramatic illustration of the many difficulties in modeling reactions.

REFERENCES

1. S. Weychant and A. Urbanek, *Int. Chem. Eng.*, **9**, 396 (1969).
2. G. Honti, *Annales du Genie Chimique, Congress Int'l. du Soufre*, Toulouse, May 22–26, 1967.
3. P. Mars and J. G. H. Maessen, *J. Catal.*, **10**, 1 (1968).

4. A. Simecek, B. Kadlec, and J. Michalek, *J. Catal.*, **14**, 287 (1969).
5. P. Mars and J. G. H. Maessen, 3rd International Congress on Catalysis, Vol. I, p. 266, Amsterdam, 1964.
6. B. Kadlec, J. Michalek, and A. Simecek, *Chem. Eng. Sci.*, **25**, 319 (1970).
7. A. Simecek, *J. Catal.*, **18**, 83 (1970).
8. S. Minhas and J. J. Carberry, *Brit. Chem. Eng.*, **14** (6), 799 (1969).
9. Regner, A. and A. Simecek, *Coll. Czech. Chem. Comm.*, **33**, 2540 (1968).
10. JANAF *Thermochemical Tables*, 2nd Ed. National Bureau of Standards, Washington, D.C., 1971.
11. H. Z. Hurlburt, *Monitoring Contact Acid Plant Converters*, 71st American Institute of Chemical Engineers, National Meeting, Dallas, Tex., Feb. 20-23, 1972.
12. B. Kadlec and V. Pour, *Coll. Czech. Chem. Comm.*, **33**, 2526 (1968).
13. B. Kadlec and A. Regner, *Coll. Czech. Chem. Comm.*, **33**, 2388 (1968).
14. H. Livbjerg and J. Villadsen, *Chem. Eng. Sci.*, **27**, 21 (1972).
15. H. Livbjerg, K. F. Jensen, and J. Villadsen, *J. Catal.*, to be published (1976).